



# QUANTITATIVE ANALYSIS ON CELLULAR UPTAKE OF LANTHANUM OXIDE NANOPARTICLES IN THE PRIMARY OSTEOSTROBLASTS IN VITRO

Yanyan Ma, Zhu Liu, Yunfei Li, Demin Zhu, Da Wang, Wenying Wang, Zhilin Li\*, Guoqiang Zhou\*

**Keywords:** Rare earth metal oxides; Lanthanum oxide nanoparticles; Cellular uptake; Osteoblasts; Nanotoxicity

With the fast developing nanotechnology, questions are being raised about the potential toxic effects of the nanomaterials on human health. The effects of lanthanum oxide nanoparticles on the primary osteoblasts are investigated in the present study. As an indicator of membrane damage, lactate dehydrogenase is quantitatively assessed. The quantitative analysis on cellular uptake of lanthanum oxide nanoparticles could be detected by flow cytometer and inductively coupled plasma mass spectrometry respectively. The results demonstrate that lanthanum oxide nanoparticles can enter cells through cell membrane and the nanoparticles taken up by the cells followed dose and time dependent effect. The method could be used for the initial screening of the uptake potential of nanoparticles as an index of nanotoxicity.

\*Corresponding Authors

E-Mail: lizhilin@hbu.edu.cn, zhougq1982@163.com  
Key Laboratory of Chemical Biology of Hebei Province,  
College of Chemistry and Environmental Science, Hebei  
University, Baoding, 071002, China

evaluated using cultured primary osteoblasts (OBs) in vitro. The analytical method using flow cytometer and inductively coupled plasma mass spectrometry can accurately reflect the amounts of  $\text{La}_2\text{O}_3$  taken up by cells. This method can be used for the initial screening of uptake by cells as an index of nanotoxicity.

## Introduction

The rapidly developing nanotechnology is providing a wide range of applications for nanomaterials.<sup>1</sup> Several of these have been proposed for application in fields of material, medical, biosciences, computer, and information technology.<sup>2</sup> Nanoparticles of metal oxide have attracted significant interests because of their atom-like size dependent properties.<sup>3</sup> Rare earth elements have unique physical and chemical properties due to their 4f orbital electron, such as high density, high melting point, high thermal conductance and conductivity.<sup>4</sup> Because of these unique properties, rare earths have been extensively used in medical, biomedical, electronics, and agronomic fields.<sup>5</sup> Lanthanum oxide ( $\text{La}_2\text{O}_3$ ), as one of rare earth metal oxides, has a band gap of 4.3 eV and the lowest lattice energy with high electric constant.<sup>6</sup>  $\text{La}_2\text{O}_3$  is used in several areas including electronics, fuel cells, optics, magnetic data storage, ceramics, catalysis, water treatment and biomedicine.<sup>7-9</sup>  $\text{La}_2\text{O}_3$  is used to make optical glasses and improves the density, refractive index, and hardness of the glass.<sup>10</sup> It is also used as a catalyst for the oxidative coupling of methane.<sup>11</sup> The possible applications of these materials have not been fully explored especially in the field of biomedical sciences. To the best of our knowledge, no studies have looked into the cellular uptake and potential toxicity of  $\text{La}_2\text{O}_3$  nanoparticles in cultured primary osteoblasts (OBs).

In this report, the size, morphology, structure and chemical composition of  $\text{La}_2\text{O}_3$  nanoparticles are characterized using scanning electron microscopy (SEM), X-ray powder diffraction (XRD), and dynamic light scattering (DLS) techniques. Furthermore, the cellular uptake and potential toxicity of  $\text{La}_2\text{O}_3$  nanoparticles were

## Experimental

### Materials and reagents

The Lanthanum nitrate hexahydrate ( $\text{La}(\text{NO}_3)_3 \cdot 6\text{H}_2\text{O}$ ), and urea ( $(\text{NH}_2)_2\text{CO}$ ) are the products of Kemiou Chemical Reagent (Tianjin, China). Kunming (KM) mice are procured from the Animal Center of Hebei Medical University. Dulbecco's modified Eagle's medium (DMEM) and trypsin are sourced from Gibco. 3-(4,5-dimethylthiazol-2-yl)-2,5-diphenyltetrazolium bromide (MTT), penicillin, streptomycin and cetylpyridium chloride are from Sigma-Aldrich. Fetal bovine serum (FBS) is obtained from Hangzhou Sijiqing Organism Engineering Institute. A LDH kit is obtained from the Nanjing Jiancheng Biological Engineering Institute (Jiangsu, China). All other reagents used in this study are of analytical grade.

### Preparation of $\text{La}_2\text{O}_3$ nanoparticles

The  $\text{La}_2\text{O}_3$  nanoparticles are prepared via an urea-based homogeneous precipitation process. 5 mL of  $\text{La}(\text{NO}_3)_3$  (1 M) is dissolved in 300 ml of deionized water and stirred for 15 minutes to obtain a clear solution. Next, 15 g of  $(\text{NH}_2)_2\text{CO}$  is slowly added to the clear solution of  $\text{La}(\text{NO}_3)_3$  with vigorous stirring. The resulting solution is homogenized using a magnetic stirrer at 25 °C for 1 h. This solution is heated at 95 °C for 3 h. The final precipitate is centrifuged and washed several times with water and anhydrous ethanol, and subsequently dried at 100 °C for 5 h. The obtained precursor is heat treated at 800 °C for 2 h with a heating rate of 2 °C min<sup>-1</sup>.

### Characterization of La<sub>2</sub>O<sub>3</sub> nanoparticles

The morphology and size of La<sub>2</sub>O<sub>3</sub> nanoparticles are measured by field emission scanning electron microscope (JSM-7500F, JEOL). A minute drop of nanoparticles solution is cast on to a carbon-coated copper grid and subsequently dried in air before transferring it to the microscope. X-ray powder diffraction is performed on a Bruker D8 Advance X-ray diffractometer employing Cu-K $\alpha$  radiation with 40 kV and 50 mA (D8 ADVANCE, Bruker). The size distribution of the nanoparticles in medium is evaluated by dynamic light scattering (Delsa Nano C, Beckman). Data analysis is carried out on six replicated tests.

### Cell viability assay

The primary OBs are prepared mechanically from three-days-old KM mouse calvarias following the sequential enzymatic digestion method described previously.<sup>12</sup> The viability of OBs is measured according to MTT method. In brief, OBs are seeded in 96-well culture plates at a density of  $2 \times 10^4$ /well and incubated for 24 h. After incubation, La<sub>2</sub>O<sub>3</sub> nanoparticles are added to the wells at concentrations of 5, 10, 20, and 40  $\mu\text{g mL}^{-1}$  and incubation continued for 24 h. The cells are incubated with La<sub>2</sub>O<sub>3</sub> nanoparticles for 48 h at the same concentrations. Nanoparticles are sonicated and vortexed before being added to the cells. Cells without nanoparticles are used as control group. 10  $\mu\text{l}$  of MTT solution is added to each well and the plates incubated for 4 h. The supernatant is removed and 100  $\mu\text{l}$  DMSO is added to solubilize the MTT. The absorbance at 570 nm of each well is measured with a microplate spectrophotometer (BioRad Model 3550). The cell viability is calculated according to the formula:  $\text{OD}_{\text{sample}}/\text{OD}_{\text{control}} \times 100$ .

### LDH measurement

Lactate dehydrogenase (LDH) activity in the cell medium is determined using a commercial LDH Kit. One hundred microlitres of cell medium is used for LDH analysis. Absorption is measured using a microplate spectrophotometer (BioRad Model 3550) at 340 nm. Released LDH catalyzed the oxidation of lactate to pyruvate with simultaneous reduction of NAD<sup>+</sup> to NADH. The rate of NAD<sup>+</sup> reduction is directly proportional to LDH activity in the cell medium and is measured as an increase in absorbance at 340 nm.

### Flow cytometry assay

Cells are treated with La<sub>2</sub>O<sub>3</sub> nanoparticles at several concentrations (5, 10, 20, and 40  $\mu\text{g/ml}$ ) for 24 h. Subsequently, the cells are washed three times with PBS, digested with trypsin, centrifuged and re-suspended in PBS. The amount of particles taken up by the cells is analyzed using a flow cytometer (FCM) (FACS Calibur, BD). In FCM, the laser beam (488 nm) illuminates cells in the sample stream which pass through the sensing area. The side scatter (SSC) light is the laser light scattered at about a 90° angle to the axis of the laser beam, and its intensities are proportional to the intracellular density.

### Lanthanum content analysis

Cells treated with several doses of La<sub>2</sub>O<sub>3</sub> nanoparticles are reacted with trypsin, then digested and analyzed for La content. Briefly, the cells are digested in nitric acid overnight and heated at about 160 °C the next day. At the same time, H<sub>2</sub>O<sub>2</sub> solution is used to drive off the vapor of nitrogen oxides until the solution is colorless and clear. The volume of remaining solutions is fixed to 3 ml with 2 % nitric acid. Inductively coupled plasma-mass spectrometry (ICP-MS, Thermo Elemental X7, Thermo Electron Co.) is used to analyze the La concentration in each sample. Indium of 20 ng mL<sup>-1</sup> is chosen as an internal standard element.

### Statistical analysis

Data are expressed as mean  $\pm$  standard deviation (S.D) from three independent experiments. Statistical evaluation is analyzed by a one-way ANOVA, followed by Tukey post-hoc analysis for multiple group comparisons. *P* values less than 0.05 are regarded as indicative of the statistical differences.

## Results and discussion

### Nanoparticle characterization

The SEM images provide information on the size and shape of the nanoparticles, however, it does not provide information whether the nanoparticles exist in single or aggregated forms in the culture medium. The morphology of La<sub>2</sub>O<sub>3</sub> nanoparticles is rod (Figure 1). The length of rod is about 300 nm and the diameter is about 80 nm.

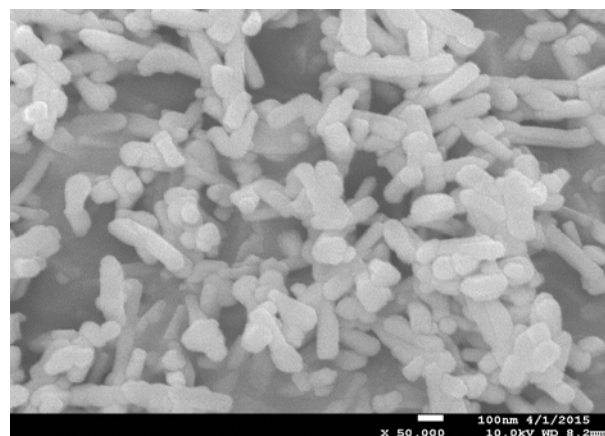
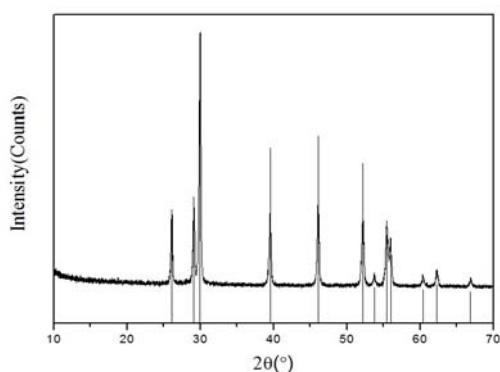
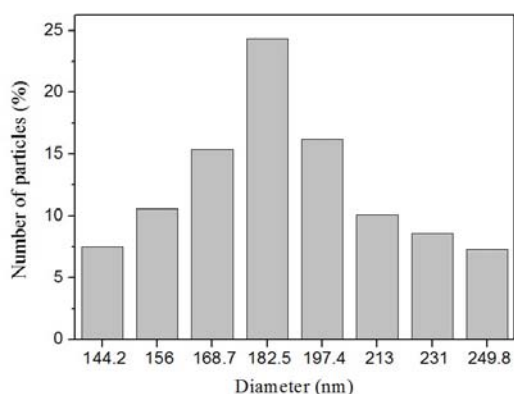


Figure 1. SEM image of La<sub>2</sub>O<sub>3</sub> nanoparticles.

The XRD patterns of La<sub>2</sub>O<sub>3</sub> nanoparticles indicate that only the La<sub>2</sub>O<sub>3</sub> phase is found without any other phase, and all diffraction peaks could be indexed to hexagonal crystal system (JCPDS No. 00-054-0213). It also reveals that La<sub>2</sub>O<sub>3</sub> nanoparticles exhibit sharp diffraction peaks, indicating a high crystallinity (Figure 2). The size distribution in the culture medium is investigated using a DLS method,<sup>12</sup> which shows that the average size of La<sub>2</sub>O<sub>3</sub> in the culture medium is  $183.5 \pm 21.3$  nm (Figure 3). The DLS analysis also shows that the La<sub>2</sub>O<sub>3</sub> nanoparticles are homogeneously dispersed in culture medium.



**Figure 2.** XRD patterns of La<sub>2</sub>O<sub>3</sub> nanoparticles.



**Figure 3.** Size distribution of La<sub>2</sub>O<sub>3</sub> nanoparticles in culture medium measured by DLS

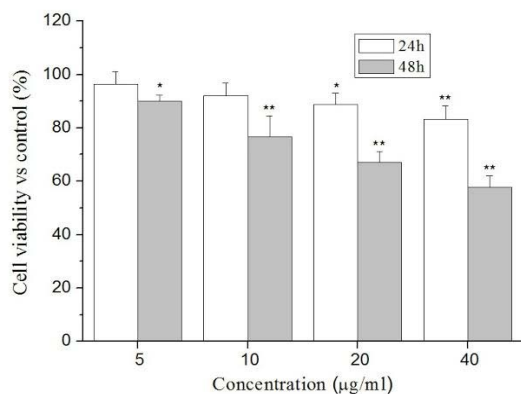


**Figure 4.** Viability of OBs after exposure to La<sub>2</sub>O<sub>3</sub> nanoparticles. Values are mean  $\pm$  SD from three independent experiments. (\* $P < 0.05$ , \*\* $P < 0.01$  compared with the corresponding control group,  $n=6$ .)

#### Effects of La<sub>2</sub>O<sub>3</sub> nanoparticles on the cell viability

The cell viability of OBs, after exposure to La<sub>2</sub>O<sub>3</sub> nanoparticles at 10, 20, and 40  $\mu\text{g mL}^{-1}$ , decreased to 92.1 %, 88.8 %, and 83.1 % respectively after 24 h, and the corresponding decrease after 48 h is 76.8 %, 67.1 %, and 57.7 % compared to the control. The inhibition effect of La<sub>2</sub>O<sub>3</sub> nanoparticles is time and dose dependent and is lower at 24 h than that at 48 h (Figure 4).

#### LDH release after exposure to La<sub>2</sub>O<sub>3</sub> nanoparticles

The cell membrane damage is reflected in the elevated LDH levels in the cell medium. The LDH levels in the cell culture increased in all groups. The increase in the cells after these have been exposed to La<sub>2</sub>O<sub>3</sub> nanoparticles at 5, 10, 20 and 40  $\mu\text{g mL}^{-1}$ , respectively for 48 h is 38.5 %, 61.5 %, 86.2 %, and 110.7 % compared with the control (Figure 5).

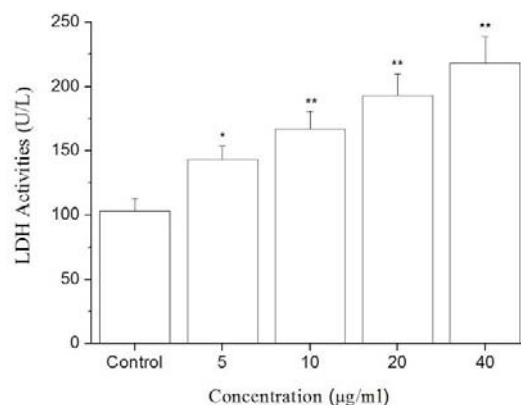


**Figure 5.** The LDH activities in the cell culture medium after exposure to La<sub>2</sub>O<sub>3</sub> nanoparticles for 48 h. Values are mean  $\pm$  SD from three independent experiments. (\* $P < 0.05$ , \*\* $P < 0.01$  compared with the corresponding control group,  $n=6$ .)

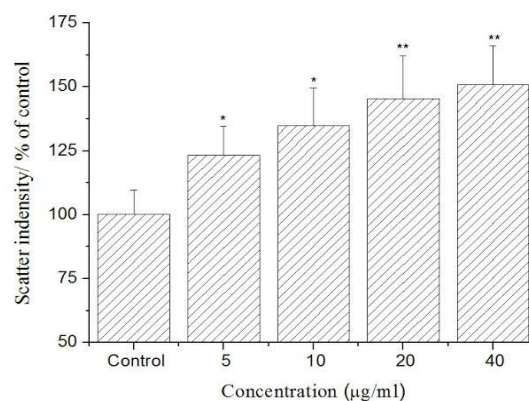


**Figure 6.** The cellular uptake of La<sub>2</sub>O<sub>3</sub> nanoparticles. The cells were incubated with different concentrations of La<sub>2</sub>O<sub>3</sub> nanoparticles for 24 h. Data are expressed as mean values  $\pm$  SD. (\* $P < 0.05$ , \*\* $P < 0.01$  compared with the corresponding control group,  $n=6$ .)

#### Flow cytometry analysis of La<sub>2</sub>O<sub>3</sub> nanoparticles uptake

The scatter intensity of La<sub>2</sub>O<sub>3</sub> nanoparticles is measured by quantitative analysis of the intracellular side scatter signal by flow cytometry. The scatter intensity increases markedly after cells are treated with nanoparticles compared with untreated group (Figure 6). The intensities of SSC reflect inner cell density and higher concentrations of La<sub>2</sub>O<sub>3</sub> nanoparticles, i.e. the cells which take up higher doses of nanoparticles show higher intensities of SSC. This result suggests that the determination of SSC is a good way to judge the uptake potential of La<sub>2</sub>O<sub>3</sub> nanoparticles. Using this experimental approach, a dose-dependent increase in cellular uptake of La<sub>2</sub>O<sub>3</sub> nanoparticles is detected at doses from 5 to 40  $\mu\text{g mL}^{-1}$  after 24 h exposure.

### ICP-MS analysis of the contents of lanthanum

ICP-MS analyses are further used to verify the uptake of  $\text{La}_2\text{O}_3$  nanoparticles in OBs at different doses and time intervals. The contents of lanthanum in cells exposed to  $\text{La}_2\text{O}_3$  nanoparticles are shown in Figure 7. Lanthanum could not be detected in controls. However, a dose- and time-dependent accumulation of  $\text{La}_2\text{O}_3$  nanoparticles are measured in OBs after 24 and 48 h. The lanthanum content of the cells, after these are exposure to  $\text{La}_2\text{O}_3$  nanoparticles at 5, 10, 20 and 40  $\mu\text{g mL}^{-1}$ , is  $8.9 \pm 0.4$ ,  $11.7 \pm 0.8$ ,  $23.8 \pm 1.1$  and  $23.6 \pm 1.2$   $\text{ng mm}^{-2}$  respectively after 24 h. The corresponding content of the cells at the same dose after 48 h of exposure increased to  $9.8 \pm 0.2$ ,  $17.1 \pm 0.7$ ,  $29.0 \pm 1.1$  and  $30.0 \pm 1.2$   $\text{ng mm}^{-2}$  (Figure 7).

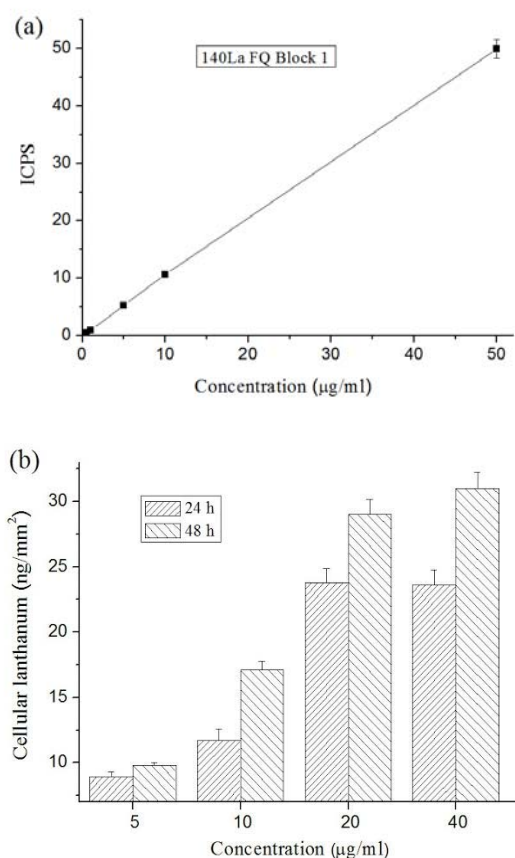


**Figure 7.** The contents of lanthanum in cells. The contents of lanthanum in cells are determined by ICP-MS. The data are expressed as mean  $\pm$  SD of three independent experiments. (a) Standard curve of the instrument. (b) The contents of lanthanum in cells.

### Conclusion

In summary, rod-like  $\text{La}_2\text{O}_3$  nanoparticles are synthesized successfully using urea-based homogeneous precipitation method. The results show that  $\text{La}_2\text{O}_3$  nanoparticles have cytotoxic effects towards primary osteoblasts.  $\text{La}_2\text{O}_3$  nanoparticles enter cells following dose and time-response effect.

At present, accurate, sensitive and cost-effective measurement techniques for characterizing them do not exist. Usage of nanomaterial will increase with the development of nanotechnology, and assessments of their risks to the environment and human health will also be required. Academia, industry, and regulatory governmental agencies should seriously consider the view that nanomaterial has new and unique biologic properties and the potential risks are not the same as those of bulk materials of the same chemistry. The simple method introduced in this study is useful for the initial screening of the uptake potential of insoluble nanomaterial in biological tissues and cells.

### Acknowledgments

This work is supported by the National Natural Science Foundation of China (21471044 and 21001038), the Youth Talent Fund Project of Hebei Education Department (BJ2014007), the College Students Innovative Training Project of Hebei University (201410075072), and the Opening Laboratory Project of Hebei University (sy2015035).

### References

- Wendelin, J. Stark., *Angew. Chem. Int. Ed.*, **2011**, *50*, 1242.
- Grainger, D. W., Castner, D. G., *Adv. Mater.*, **2008**, *20*, 867.
- Bojari, H., Malekzadeh, A., Ghiasi, M., *J. Clust. Sci.*, **2014**, *25*, 387.
- Huang, P. L., Li, J. X., Zhang, S. H., Chen, C. X., Han, Y., Liu, N., Xiao, Y., Wang, H., Zhang, M., Yu, Q. H., Liu, Y. T., Wang, W., *Environ. Toxicol. Pharmacol.*, **2011**, *31*, 25.
- Mekhemer, G. H., *Phys. Chem. Chem. Phys.*, **2002**, *4*, 5400.
- Bahari, A., Anasari, A., Rahmani, Z., *J. Eng. Technol. Res.*, **2011**, *3*, 203.
- Balusamy, B., Kandhasamy, Y. G., Senthamizhan, A., Chandrasekaran, G., Subramanian, M. S., Tirukalikundram, S. K., *J. Rare. Earth.*, **2012**, *30*, 1298.
- Nejad, S. J., Abolghasemi, H., Moosavian, M. A., Golzary, A., Maragheh, M. G., *J. Supercrit. Fluids.*, **2010**, *52*, 292.
- Khanjani, S., Morsali, A., *J. Mol. Liq.*, **2010**, *153*, 129.
- Ghiasi, M., Malekzadeh, A., *Superlattices. Microstruct.*, **2015**, *77*, 295.
- Vishnyakov, A. V., Korshunova, I. A., Kochurikhin, V. E., Salnikova, L. S., *Kinet. Catal.*, **2010**, *51*, 273.
- Zhou, G. Q., Gu, G. Q., Li, Y., Zhang, Q., Wang, W. Y., Wang, S. X., Zhang, J. C., *Biol. Trace. Elem. Res.*, **2013**, *153*, 411.

Received: 13.01.2016.

Accepted: 24.02.2016.